Regional Environmental Change (2023) 23:63
https://doi.org/10.1007/s10113-023-02039-w

ORIGINAL ARTICLE

Future changes in wind energy resources in Egypt under Paris climate agreements' goals

Ahmed Mohamed Gebaly[1] · Mohamed Salem Nashwan[1] · Wael Mohamed Hamdy Khadr[1] · Shamsuddin Shahid[2]

Received: 22 October 2022 / Accepted: 24 January 2023 / Published online: 20 April 2023
© The Author(s) 2023

Abstract

The Paris climate agreements' goals ambitiously aim to hold mean global warming below 2.0°C and to pursue efforts to limit the warming to 1.5°C. One of the effective strategies for achieving these goals and reducing greenhouse gas emissions in the energy sector is using wind power. As Egypt is heavily investing in wind farm projects and planning to depend more on wind energy resources in its energy mix, it is important to assess the impact of climate change on its future wind energy production. This study employed eight global climate models of CMIP6 to project the wind power density (WPD) changes under the shared socioeconomic pathways (SSPs) 1–1.9 and 1–2.6 that inform Paris climate agreements and SSP5–8.5 that present the extreme warming scenario. The results showed that the WPD would increase in most Egypt, except in the far southeast. Increases would be pronounced over the far western desert and in Winter compared to other seasons. Nevertheless, Summer and Fall shall have the highest WPD by the end of the century compared to the present. This is favorable because the seasonal WPD pattern is sufficient to meet the local energy need. Unlike the intra-annual variability, few changes were projected in the inter-annual variability of WPD. Furthermore, a shift towards stronger WPDs compared to the historical period was observed. This study's results can be useful for energy policymakers and planners in managing wind energy production under climate change scenarios.

Keywords CMIP6 · Projection · Renewable energy · MENA · Wind · Climate

Introduction

Renewable energy plays a fundamental role in mitigating the drastic increase in atmospheric greenhouse gases (GHGs). Countries worldwide have strategically planned to depend more on renewable energy production. Egypt has set a target to supply 42% of the country's electricity mix by 2035 from renewables (IRENA 2018). Implementation of solar and wind energies is more realistic and cost-effective in Egypt than other renewables. Reports indicate 53% of its electricity supply from solar and wind energies by 2030 is realistic and cost-effective (IRENA 2018). Out of different renewables, wind energy has grown rapidly since 2000 due to technological maturation, declining cost, and supportive policies, making it the 2nd in terms of installed energy-generating capacities worldwide (IRENA 2022). Currently, wind energy production in Egypt accounts for 1375 MW which is 12% of total electricity consumption (Bissada 2021; IRENA 2018; NREA 2021).

Although wind energy production is a key player in mitigating climate change, wind power is very susceptible to climate change itself. The expected variation in wind magnitude shall definitely alter wind energy generation. Moreover, the wind energy potential has a cubed correlation with wind speed. Thus, a small variation in wind speed heavily changes energy production, impacting the wind energy industry's reliability, stability, and profitability. As governments worldwide shall depend more on wind energy in their future energy mix, it is vital to assess the changes in future production. Furthermore,

Communicated by Wolfgang Cramer.

✉ Mohamed Salem Nashwan
m.salem@aast.edu

Ahmed Mohamed Gebaly
ahmedgebaly92@gmail.com

Wael Mohamed Hamdy Khadr
wkhadr@aast.edu

Shamsuddin Shahid
sshahid@utm.my

[1] Department of Construction and Building Engineering, Collage of Engineering and Technology, Arab Academy for Science, Technology and Maritime Transport (AASTMT), Elhorria, Cairo 2033, Heliopolis, Egypt

[2] School of Civil Engineering, Faculty of Engineering, Universiti Teknologi Malaysia (UTM), 81310 Skudai, , Johor, Malaysia

wind farms and supporting infrastructure are expensive to construct. Therefore, it is crucial to evaluate the future potential in wind energy generation at the current wind farm locations and the potential of other locations for wind energy generation.

Future climatic conditions can be investigated by employing Global Climate Models (GCMs), as they can simulate the effect of varying GHG emission levels on our climate system. The Scenario Model Intercomparison Project (ScenarioMIP) within the Coupled Model Intercomparison Project phase 6 (CMIP6) is currently the newest state-of-art climate projection that incorporates different scenarios of social concerns related to adaptation, mitigation, and impact of climate change (Riahi et al. 2017). These projections in CMIP6 are derived for new future pathways, Shared Socioeconomic Pathways (SSPs), that integrate possible changes in radiative forcing, GHG emissions, technological development, and global social, economic, and political scenarios. The CMIP6 models can represent earth's physics more accurately. Several studies have reported the better performance of CMIP6 GCMs over the previous CMIPs in Asia (Hamed et al. 2022c; Song et al. 2021), Europe (Di Sante et al. 2021; Nie et al. 2020; Palmer et al. 2021), North America (Bourdeau-Goulet and Hassanzadeh 2021; Ortega et al. 2021), and Africa (Ayugi et al. 2021; Hamed et al. 2022b; Nashwan and Shahid 2022). Out of the eight available SSPs (Meinshausen et al. 2020), SSP1–1.9 and SSP1–2.6 address the Paris climate agreement goals of limiting global warming to < 2.0°C above the pre-industrial era (1850–1900) and to pursue efforts to limit the warming to < 1.5°C, respectively (UNFCCC D, 2015).

Bloom et al. (2008) analyzed the change in wind energetic resources over Eastern Mediterranean using the Had3CM of CMIP3 for A2 scenario and found an overall rise in wind resources over land and a reduction over the sea, except for the Aegean Sea, during 2071 to 2100. They demonstrated that eastern Egypt wind speeds were undervalued by 2.5 ms^{-1} in Winter and overvalued by 2.5 ms^{-1} in Summer in the Suez Gulf regions. Carvalho et al. (2017) projected the expected changes in wind resources over Europe for two CMIP5 scenarios (RCP4.5 and 8.5) using a multimodel ensemble (MME) and showed that all European territories would experience a drop in the wind resources, except in the Baltic Sea, for RCP8.5. Carvalho et al. (2021) continued their previous research by analyzing the difference in projections of wind recourses between CMIP5 and 6. They showed a strong decrease in wind resources all over Europe, in the Baltic Sea, by the end of 2100 for SSP5–8.5. However, CMIP6 GCMs projected a high increase in wind resources during summer in southern Europe and the far north of Egypt, whereas CMIP5 projected the opposite. Sawadogo et al. (2021) projected the changes in wind energy potential for two CMIP5 emission scenarios using Regional Climate Model version 4 (RegCM4) and reported a max increase of 20% in the near and mid-century for both RCPs. They also stated a higher increase in wind energy for RCP2.6 than RCP8.5 in Africa. Akinsanola et al. (2021) found that wind resources will increase by up to 70% on the Guinea coast, West Africa, and significantly decrease over the Sahel subregion using CMIP6 GCMs. Davy et al. (2018) projected an increase in wind resources over North Africa for RCP4.5 and 8.5 using the Rossby Centre, RCA4 regional climate model under the European domain of Coordinated Regional Climate Downscaling Experiment (CORDEX).

No previous studies assessed Egypt's future wind energy potential under climate change scenarios. Only a few studies assessed the historical change in wind speed in some regions using meteorological records. Lashin and Shata (2012) suggested the high potential of wind power generation in Port Said, northeast of Egypt, especially in Spring, using historical wind speed observation (1991–2005). Effat (2014) pointed out that the Red sea zone, especially the northern parts (i.e., Gulf of Suez), has a high potential for wind power generation. They mapped rich wind power potential zones avoiding sensitive ecological sites using remotely sensed data and a GIS-based model. Ahmed (2018) studied the wind energy potential of Sharq El-Ouinat (south of Egypt) using a shorter period (2001–2005) wind speed record and revealed its high potential.

It can be clearly understood from the previous review that little is known about the future state of wind energy potential in Egypt. This study's objective is to assess the response of future wind energy resources in Egypt under the emission reduction scenarios of the Paris climate agreements' goals. The output of eight GCMs for SSP1–1.9 and SSP1–2.6, which simulate the agreement goals, was utilized to form MMEs and project changes in annual and seasonal wind energy potential and their geographical distribution. Furthermore, the results were compared to that obtained for the high-emission scenario, SSP5–8.5, representing the upper boundary of global climatic change in the case of fossil-fueled development and limited measures to decrease GHG emissions. The results of this study shall be helpful for Egyptian energy policymakers in planning and management of future wind energy productions.

Study area

Egypt is located in the far northeastern of the African continent linking Africa to Asia by the Sinai Peninsula. Its land area is approximately one million km^2, with a 3500 km coastline along the Mediterranean and Red Seas. As seen in supplementary Fig. S1, the Nile River enters Egypt from the south and flows to the north, splitting Egypt into Eastern and Western deserts. Egypt has mostly flat topography except for the mountain chains along the

Red Sea and in Sinai. Summers in Egypt are hot and dry, while winters are chilly and rainy. Warm dry air usually comes from the east, especially the Arabian Peninsula. In opposition, cold winds usually are northerly and northwesterly cold advection from Europe (El Kenawy et al. 2019a, b; Hamed et al. 2022a).

Egypt has many promising wind projects, such as the Zafarana wind farm (labelled no. 1 in supplementary Fig. S1) with 700 wind turbines and a total capacity of 545 MW, Gabal El Zeit wind farm (no. 2) with a total capacity of 580 MW, and Suez Gulf first privately owned wind farm (no. 3) having a capacity of 250 MW. In addition, Egypt has planned several projects in the Suez Gulf with a total capacity of 2400 MW, such as the West Bakr wind farm (no. 4) with a capacity of 250 MW (NREA 2021).

Data and sources

The present study aims to assess the effect of climate change on wind power density in Egypt for the Paris climate agreements' goals. It employed the available eight CMIP6 GCMs, as listed in Supplementary Table S1, having the monthly u and v wind components for the present time climate and different future scenarios. The future scenarios used were SSP1–1.9, SSP1–2.6, and SSP5–8.5. SSP1–1.9 and SSP1–2.6 are new scenarios in CMIP6 that inform the Paris climate agreements' targets, contain little CO_2 and GHG emissions decreasing to almost net-zero by the mid-century, subsequently net negative CO_2 emission (IPCC 2021). The SSP1–1.9 simulates a global warming pathway that would not exceed 1.5°C beyond pre-industrial levels by 2100 (Rogelj et al. 2018). Meanwhile, the SSP1–2.6 pathway is designed for 1.8°C warming by the end of the century (Meinshausen et al. 2020; Rogelj et al. 2016). Furthermore, SSP5–8.5 was used as a benchmark for comparing the results obtained for the Paris climate agreements' goals. SSP5–8.5 is the worst-case scenario containing very high GHG emissions. Hamed et al. (2022d) found that bias in CMIP6 wind speed components in Egypt is very low (± 1 m/s) compared to the European reanalysis ERA5. Furthermore, the uncertainty in CMIP6 projections is relatively narrower than that for the CMIP5 (Hamed et al. 2022d).

Methodology

Data processing

The GCM simulated u and v components of wind at 10 m (U10) were used to estimate wind speed at each grid location. GCMs outputs were presented on different raw spatial distributions, as shown in supplementary Table S1. Thus, the wind speed estimates at raw resolution were remapped into a common $1° \times 1°$ grid (approximately the average of the resolution CMIP6 GCMs) using a bi-linear interpolation technique. The bi-linear interpolation technique is commonly used to interpolate GCM outputs as it does not interfere with the climate change signal (Nashwan et al. 2020; Salman et al. 2020). The re-gridded wind speed data of different GCms were used to develop MME. The MME U10 for 1990–2014 were compared to European Reanalysis 5 (ERA5) U10 to assess its performance. Pearson's correlation (r), percentage of bias (%bias), and the Kling-Gupta efficiency (KGE) metrics were used as the evaluation metrics. The optimal r and KGE are one and zero for the %bias. The ERA5 was used for comparison as it is the latest and most advanced reanalysis produced by European Centre for Medium-Range Weather Forecasts (ECMWF). It incorporates the Integrated Forecasting System (IFS) cycle 41r, ground observations, and remote sensing data to develop its climate estimates. ERA5 was found to reproduce the regional climate of Egypt accurately (Gleixner et al. 2020; Hamed et al. 2021).

Since wind turbines are usually installed at 80 to 120 m above the ground elevation (or mean sea level for offshore turbines), the 10 m wind speed estimates were extrapolated to 100 m height (average wind turbine level). Wind speed extrapolation is commonly conducted using either the wind power law or logarithmic wind profile. From 100 m to the near top layer of the atmosphere, more accurate estimations of wind speed are expected using the wind power law (Pryor et al. 2005). Thus, it was used to extrapolate wind speed to 100 m using Eq. (1).

$$\frac{U_z}{U_{z_r}} = \left(\frac{z}{z_r}\right)^{\alpha} \tag{1}$$

where U_z is the wind speed at target level z (here, 100 m), U_{z_r} is the wind speed at a reference level z_r (here, 10 m), and α is the power-law exponent (here, 0.14 following the International Electrotechnical Commission recommendation for inshore).

Wind energy resources

The $1° \times 1°$ 100 m wind speed estimates were used to calculate the magnitude of wind power density (WPD) for each GCM for the historical (1990–2014) and future (2041–2100) periods to characterize wind energy resources. The WPD is a widely used metric for assessing wind energy resources as it allows the comparison among the potential of different locations in wind energy resources independent of turbines' power curves (Cook 1985; Costoya et al. 2020a). WPD is the wind power in the unit area ⊥ to the airflow (Eq. 2).

$$\mathrm{WPD} = \frac{\rho v_i^3}{2} \tag{2}$$

where WPD is in Wm^{-2}, ρ is the air density in kgm^{-3}, and v_i is the 100 m wind speed in ms^{-1}. The air density was calculated using Eq. (3).

$$\rho = \frac{P}{RT} \tag{3}$$

where P is the average sea level pressure in Pa, R is the gas constant, and T is the average temperature in °Kelvin. Here, the ERA5 data of P and T were used to calculate the average areal ρ of 1.19314 kgm^{-3} for Egypt for the historical period. This value was assumed to be the same in the future.

Changes in projected wind power density and assessment of uncertainty

The calculated WPDs for all GCMs were used to generate MME to assess the changes in WPD due to climate change. The future changes in WPD were estimated as the percentage difference between the MME mean of future WPD and the MME mean of historical WPD. The changes were calculated for the annual average and seasonal WPD. The credibility of the climate change signal was assessed based on how each GCM agreed with the sign of MME mean change. A robust/consistent climate change signal was annotated when ≥ 75% of the MME member agreed on the sign of the change. Meanwhile, a not-credible change signal was annotated when ≤ 25% of the members agreed. The credibility of the change signal was assessed at each grid point, and the grids having robust (not credible) signals were marked.

The probability distribution function skill score (PDFss) was used to assess the change in distribution in monthly WPD. The PDFss, proposed by Perkins et al. (2013), is a measure of the overlap between a couple of probability distribution functions by computing the cumulative minimum value of their distributions (Eq. 4). The score values can range between zero and one, where one designates a perfect PDF overlap. However, unlike previous studies, the PDFss was used in this study to assess the projected distributional changes between the historical WPD and future estimates. Thus, the difference in PDFss (1-PDFss) was calculated to give these changes a quantitative score.

$$\mathrm{PDF_{SS}} = \sum_{1}^{n} \min(M_y, M_x) \tag{4}$$

where M_y and M_x are the ratios of values for a given n of bins from the historical and future probability distribution functions.

Furthermore, this study employed the Robust Coefficient of Variation (RCoV) to understand the variability in wind power at intra-annual and inter-annual scales. The RCoV is the ratio of the median absolute deviation (MAD) to the median time series of WPD, as expressed in Eq. 5. The intra-annual RCoV was computed for each grid point (i) as follows: (1) the monthly time series of MME mean of WPD were constructed for the historical and future periods; (2) the median WPD and MAD were computed for each year; (3) the division of the annual MADs was computed as the ratio of the annual RCoV to the corresponding annual median WPD; finally, (4) the median of the annual RCoV was calculated and presented in the "Results" section. The same procedure was carried out to calculate the inter-annual variability of WPD but using the annual mean WPD instead of the monthly mean. Besides, the RCoV was computed using the annual mean MME time series.

$$RCoV = \frac{MAD}{Median} = \frac{median\left[\left|WPD_i - median\left(WPD_i\right)\right|\right]}{median(WPD_i)} \tag{5}$$

Results

The mean annual wind speed and direction at 10 m high over Egypt for the base period (1990–2014) as estimated by the MME is presented in supplementary Fig. S2. It shows that high wind speeds were concentrated in Egypt's center, which gradually increased to the maximum in the central south. The wind in the northwest ranged from 2.17 to 4.18 ms^{-1}. On the other hand, the lowest wind speed was in the east of Egypt. The MME U10 averaged for the base period was compared to the averaged ERA5 to evaluate the MME performance. Fig. S2 (b) shows that the MME can reproduce ERA5 data adequately, as most points are aligned along the 1:1 diagonal line. The statistical assessment revealed $r = 0.85$, %bias = 4.3%, and KGE = 0.63 for MME U10.

The wind speed at 10 m height was then converted to 100 m height. The WPDs for the historical and future periods were then computed to estimate the changes in WPDs for different SSPs. Figure 1 displays the annual and seasonal averages of WPD for the historical period (1990–2014). The results showed that the spatial distributions of WPD for different timeframes were similar to that of wind speed presented in Fig. S2. The WPD in the central south had the highest magnitude, and the east had the lowest. Figure 1 also shows that the annual WPD ranged from 7 to 218 Wm^{-2}. Among different seasons, Fall (August to October) had the highest WPD (mean 92 Wm^{-2}), and Winter (November to January) had the lowest (mean 27 Wm^{-2}). WPD in Fall and Winter ranged from 37 to 218 Wm^{-2} and 7 to 87 Wm^{-2}, respectively. It ranged from 10 to 90 Wm^{-2} in Spring

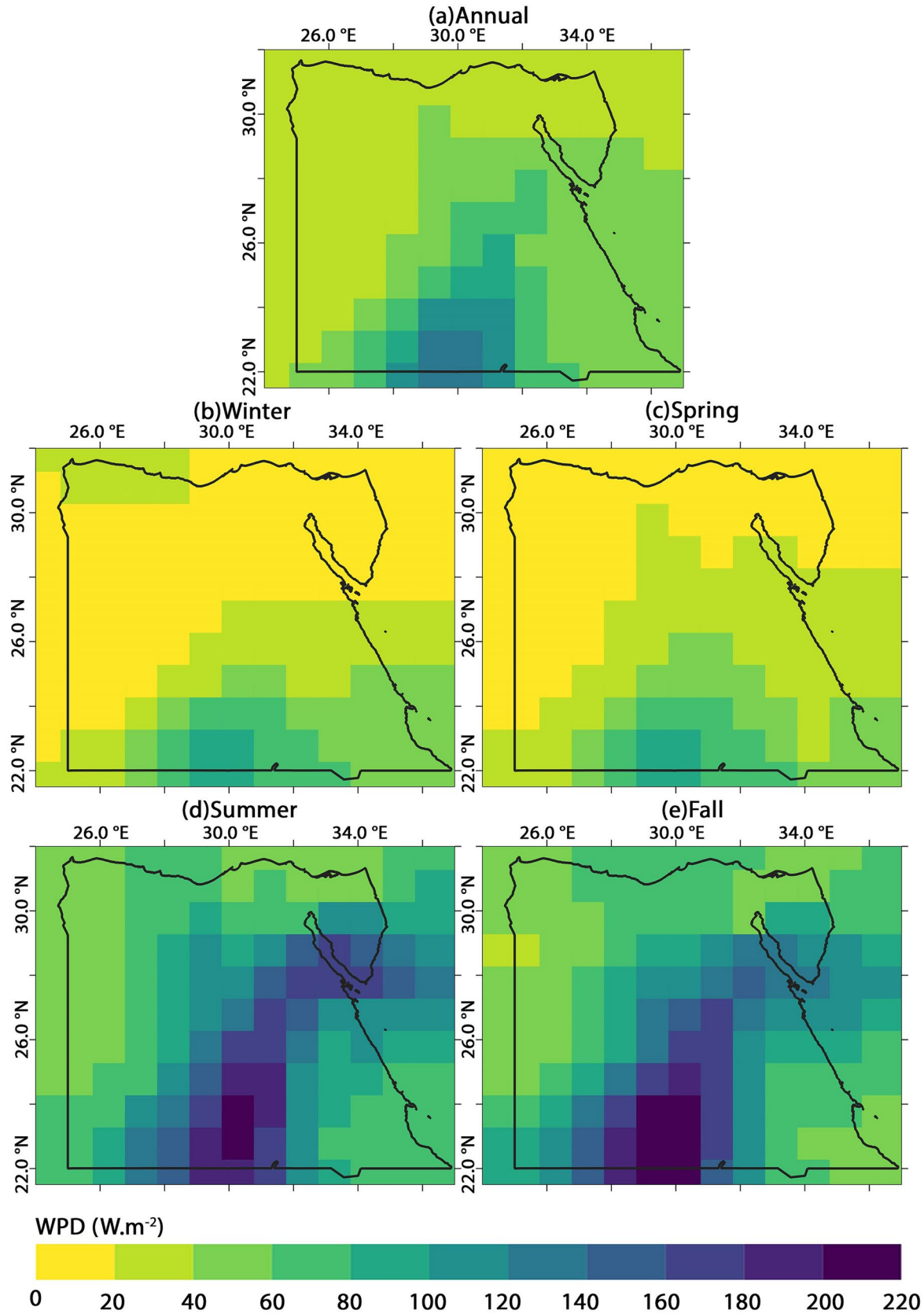

Fig. 1 Average wind power densities in Egypt for annual and seasonal timeframes during the historical period (1990–2014)

(February–April) and 45 to 206 Wm^{-2} in Summer (May, June, and July).

Figure 2a–d demonstrates the time series of projected WPD for SSP1–1.9, 1–2.6, and 5–8.5. The intermediate black dashed lines represent the MME mean WPD, and the bands represent MME projections' 90th percentile confidence intervals. The figure reveals no significant difference in the year-to-year WPD variability of different SSPs. It also shows that the confidence bands are mostly narrow. The fluctuations were more for the upper than the lower confidence level. The average bandwidths were 65.6, 62.9, and 68.7 Wm^{-2} for SSP1–1.9, SSP1–2.6, and SSP5–8.5, respectively. This reflects the small inner-model variability. The figure also shows the difference between the mean projected and historical WPD. The SSP1–2.6 (the blue line) showed a declining trend with the lowest difference (average of 1.1 Wm^{-2}) and the highest negative change (− 9.6 Wm^{-2}, in 2100). In contrast, SSP5–8.5 (the red line) showed a rising trend with the highest difference (average of 4.1 Wm^{-2}) and the highest positive change (16.6 Wm^{-2}, in 2099). Furthermore, the difference for SSP1–1.9 (green line) was in the middle of the other two SSPs, with no notable trend (ranges between 10.8 and − 3.6 Wm^{-2}) with an average difference of 2.2 Wm^{-2}.

Figure 3 shows the projected annual WPD (%) changes over the study area for three SSPs during 2041–2100. It revealed that plenty of the change signals are robust (i.e., most MME members agree on the sign of the change) with no unrealistic signals within the study area. The results showed that most of Egypt would experience varying levels of increase in WPD for different SSPs, except in the far southeast. The average overall changes were 8.8, 10.1, and 14.2% for near, mid, and far futures, respectively. The WPD was projected to increase in the west of Egypt up to 16.3, 12.8, and 29.2% in the near future, 12.9, 14.3, and 41.3% in mid-future, and 11.0, 15.5, and 67.7% in the far future for SSP1–1.9, SSP1–2.6, and SSP5–8.5, respectively. The higher WPD was projected in the Suez gulf area by 11.7, 8.5, and 16.7% in the near future, 8.6, 8.6, and 24.2% in the mid-future, and 7.3, 8.3, and 39.3% in the far future for the three SSPs. However, 9.0% of Egypt, mainly in the far northwest and southeast, would experience a reduction in WPD by 2.3% during 2041–2060 for SSP1–2.6. The higher decrease in WPD (10.5% of total area) would be for SSP1–1.9 during 2081–2100. However, it would be much smaller for SSP5–8.5 and SSP1–2.6 (1.0 and 0.9%) for the same period.

Figure 4 illustrates the projected changes (%) in seasonal WPD in the near future (2041 to 2060). The major changes in both directions (+ ve and − ve) would be in Winter for all scenarios. However, most negative change signals were unrealistic, except for Summer and Fall for SSP5–8.5. Most areas having positive change signals were robust. WPD changes in Winter may reach 44.1 and 35.4% for SSP1–1.9 and SSP1–2.6, respectively. It may increase to a maximum of 77.6% for SSP5–8.5, which is the highest for all seasons. Spring showed the most credible change signals, primarily positive, except for the far northwest. The changes in Spring were − 3.0 to 30.9%, − 6.9 to 23.2%, and 7.1–56.9% for the three SSPs. Figure 4 shows the lowest changes in Summer than in other seasons. A reduction in WPD will be experienced over the largest areas (42.6% of the study area) in Summer. Non-credible signals were found in the southeast of Egypt for SSP1–2.6. However, most were out of the study area for SSP1–2.6 and a few points in the far northwest for SSP5–8.5. The far north of Egypt would experience more WPD change, by 16.1, 9.8, and 7.1% for the three SSPs. The future changes during Fall would be − 7.2 to 13.9%, − 10.4 to 16.1%, and − 9.4 to 25.6% for SSP1–1.9, 1–2.6, and 5–8.5 with non-credible signs for SSP1–2.6, mainly in the eastern areas outside the Egyptian borders.

Figure 4 also illustrates the projected seasonal changes (%) during 2061−2080. Winter showed the major differences, both positive or negative, for all scenarios. Still, the majority of the negative change signals were not found credible. Most areas with positive change signals were found robust. The increase may reach 41.0% and 51.0% for SSP1–1.9 and SSP1–2.6, respectively. For SSP5–8.5, the increase may reach a maximum of 138.6%, which is the greatest overall change. The most credible change signals, which are mostly positive, were noticed in Spring. The changes in Spring were − 1.2 to 33.8%, 1.9–32.1%, and 12.6–93.8% for the three SSPs. Figure 4 displays the least changes in Summer than in other seasons. Non-credible signals were noticed in different regions for different SSPs. The far northwest of Egypt would have 7.0, 6.4, and 20.7% more WPD for the three SSPs. The future changes during Fall would be − 3.7 to 10.3%, − 6.1 to 13.0%, and − 8.4 to 36.4% for SSP1–1.9, 1–2.6, and 5–8.5, respectively. Most of the study areas showed credible signs for SSP5–8.5.

The projected changes (%) in seasonal WPD by the end of the century (2081–2100) for different scenarios were very similar to that obtained for the period 2061–2080. However, the increase in Winter WPD was more for SSP5–8.5 (203.0%) during 2080–2100 than 2061–2080. The results are provided in supplementary Fig. S3.

Figure 2e–g presents the probability density functions (PDFs) of future projections of monthly WPD for different SSPs in comparison to monthly historical estimates. The results showed a shift in the peak of the PDFs towards stronger WPDs compared to the historical period with lower probability densities regardless of the future timeframes. This shift was measured for different SSPs and periods using 1-PDFss. Supplementary Table S2 shows the biggest shift for SSP5–8.5, which also increased with time. SSP1–1.9 showed the lowest shift. Furthermore, SSP1–1.9 and SSP1–2.6 would have a comparable distribution of WPD at the end of the century.

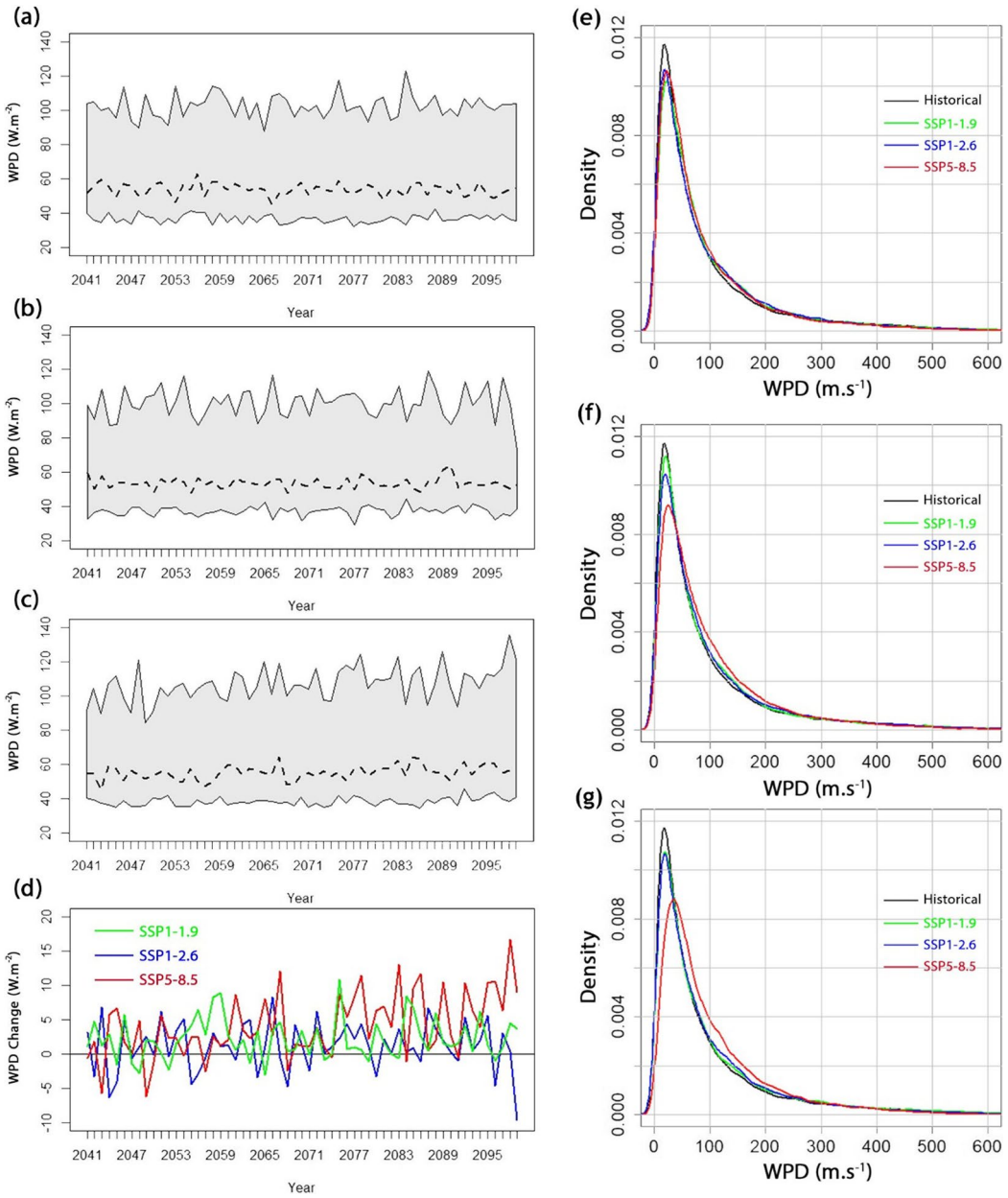

Fig. 2 Future wind power densities time series (**a**–**d**) and probability distribution functions (PDFs, **e**–**g**). Time series of future wind power densities (Wm.$^{-2}$) from 2041 to 2100 for **a** SSP1–1.9, **b** SSP1–2.6, and **c** SSP5–8.5, and **d** the difference between the shared socioeconomic pathways and mean wind power densities of the historical period. PDFs of monthly historical wind power densities and its future projections for different shared socioeconomic pathways during **e** 2041–2060, **f** 2061–2080, and **g** 2081–2100

Figure 5 presents the spatial patterns in the inter-annual RCoV, which was used to analyze variation in monthly WPD across Egypt for different timeframes. The higher the RCoV, the larger the variability in WPD. The figure shows that the highest RCoV were mainly in the Gulf of Suez and Sinai, pointing to wide inter-annual variability for all periods. The intra-annual variability in the present and future climates gradually decreased and generally became lowest in the southeast. The average inter-annual RCoV was 0.43–1.22 for the historical period. Those were 0.38–1.09, 0.36–1.17, and 0.37–1.18 for SSP1–1.9 and 0.48–1.25, 0.40–1.17, and 0.43–1.19 for SSP1–2.6 in the near, mid, and far futures, respectively. A slight change was observed for SSP5–8.5 compared to SSP1–1.9. The average RCoV was 0.42–1.18, 0.44–1.20, and 0.40–1.13 for the three future periods. The middle south and southeast would experience low variability. Meanwhile, the northeast would experience the highest variability for all periods and scenarios.

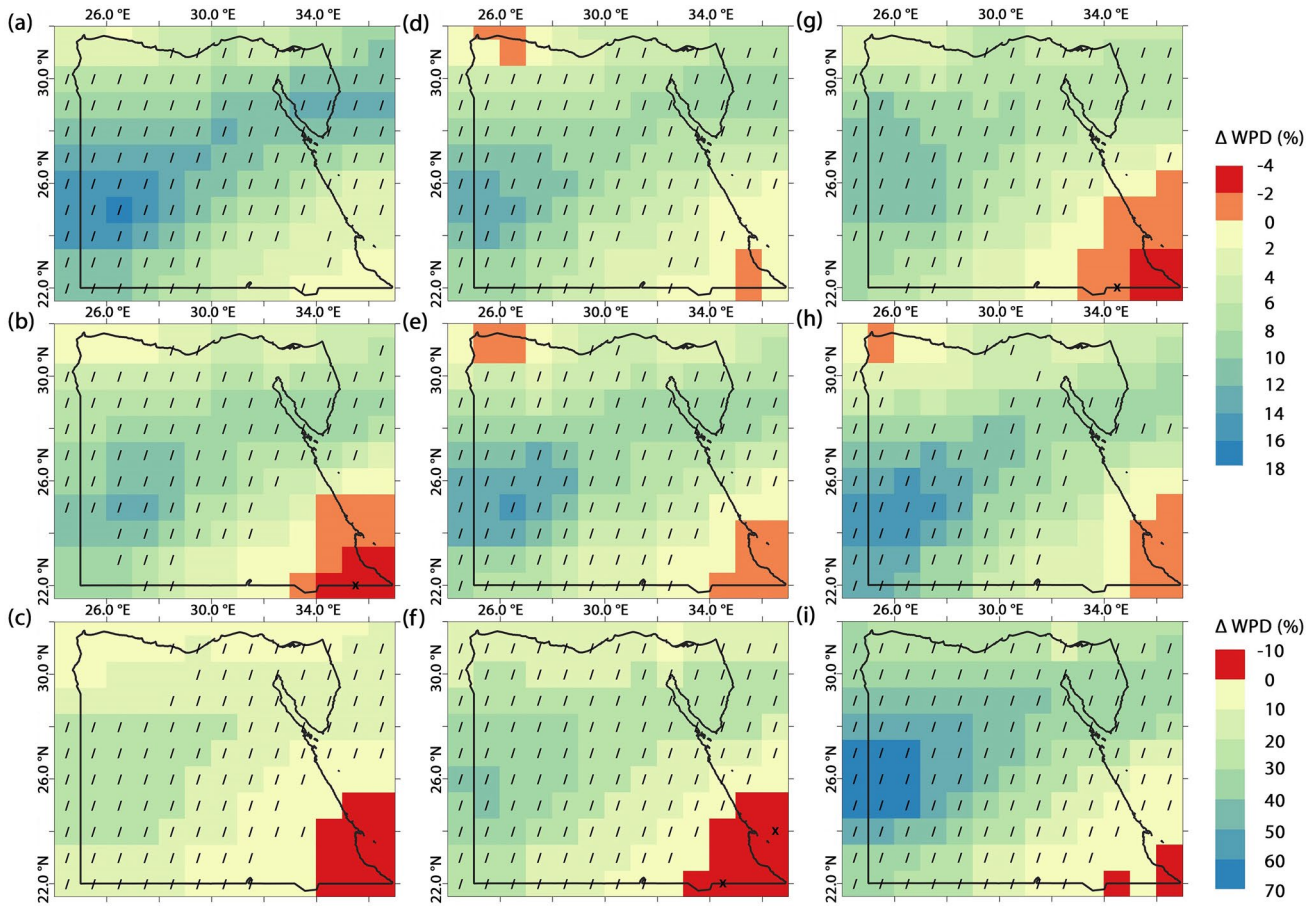

Fig. 3 Changes (%) in annual wind power densities (WPD) during 2041–2060, 2061–2080, and 2081–2100 (columns) for SSP1–1.9, SSP1–2.6 and SSP5–8.5 (rows)

The intra-annual RCoV for the historical and three future periods for different SSPs is presented in supplementation Fig. S4. Generally, small RCoV was observed for different timeframes, which means low year-to-year variation in WPD across Egypt. The average intra-annual RCoV was 0.047–0.108 for the historical period, while 0.022–1.00, 0.027–0.090, and 0.027–0.111 for SSP1–1.9, 0.044–0.138, 0.033–0.114, and 0.024–0.106 for SSP1–2.6, and 0.018–0.097, 0.028 0.093, and 0.028–0.12 for SSP5–8.5 in the near, mid, and far futures. Overall, the northwest would experience a high variability and the middle south the least.

Discussion

This study investigated the impact of global warming on the generation potential of wind power over Egypt for different future spans using an ensemble of CMIP6 GCMs. The GCMs estimated the wind status for three SSPs that simulate global warming below 1.5 and 2.0°C by the end of the century (i.e., SSP1–1.9 and 1–2.6) as well as the worst-case impact of climate change (SSP5–8.5). The results showed that the WPD would increase for most Egypt, except in the far southeast. Increases were pronounced over the far western desert and in Winter compared to other seasons. Nevertheless, Summer and Fall would have the highest WPD by the end of the century, like in the present. This is favorable as seasonal WPD is equal to the local energy usage (Abubakr et al. 2022; Osman et al. 2009). Unlike the intra-annual variability, few observed changes were projected in the inter-annual variability of WPD for most of Egypt. Therefore, the same spatial distribution of RCoV was observed for different scenarios and future spans. Furthermore, the results revealed a shift in the peak of the PDFs towards stronger WPDs compared to the historical period.

As reviewed in the introduction, limited studies explored Egypt's potential changes in wind speed or power due to global warming. However, this study's results agree with Sawadogo et al. (2021) in the increase in WPD over Egypt, where they projected a similar increase over north Africa but for RCP2.6 and 8.5 using RegCM4 CORDEX-CORE

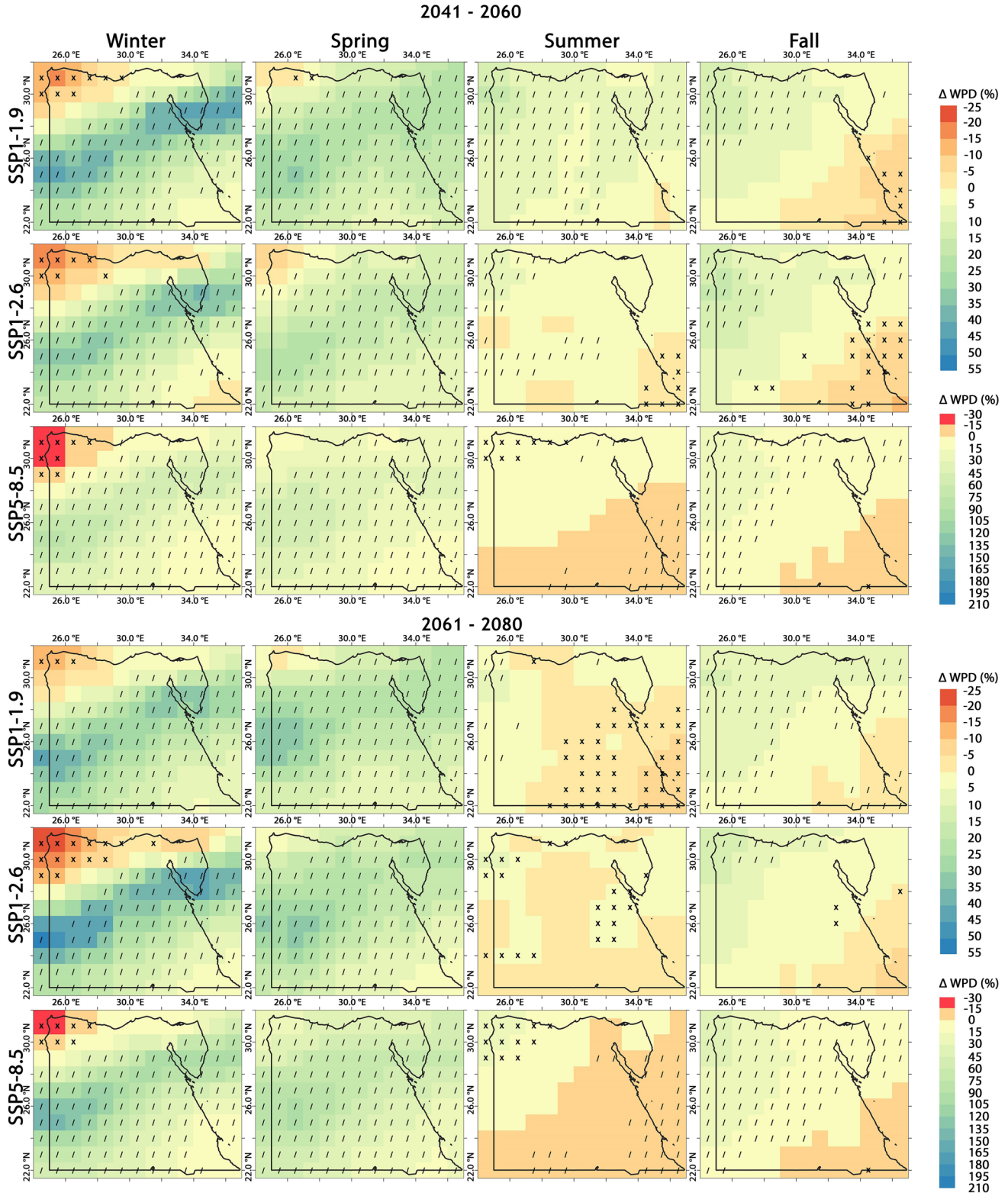

Fig. 4 Projected changes (%) in seasonal wind power densities (columns) for different shared socioeconomic pathways (rows) during 2041–2060 and 2061–2080

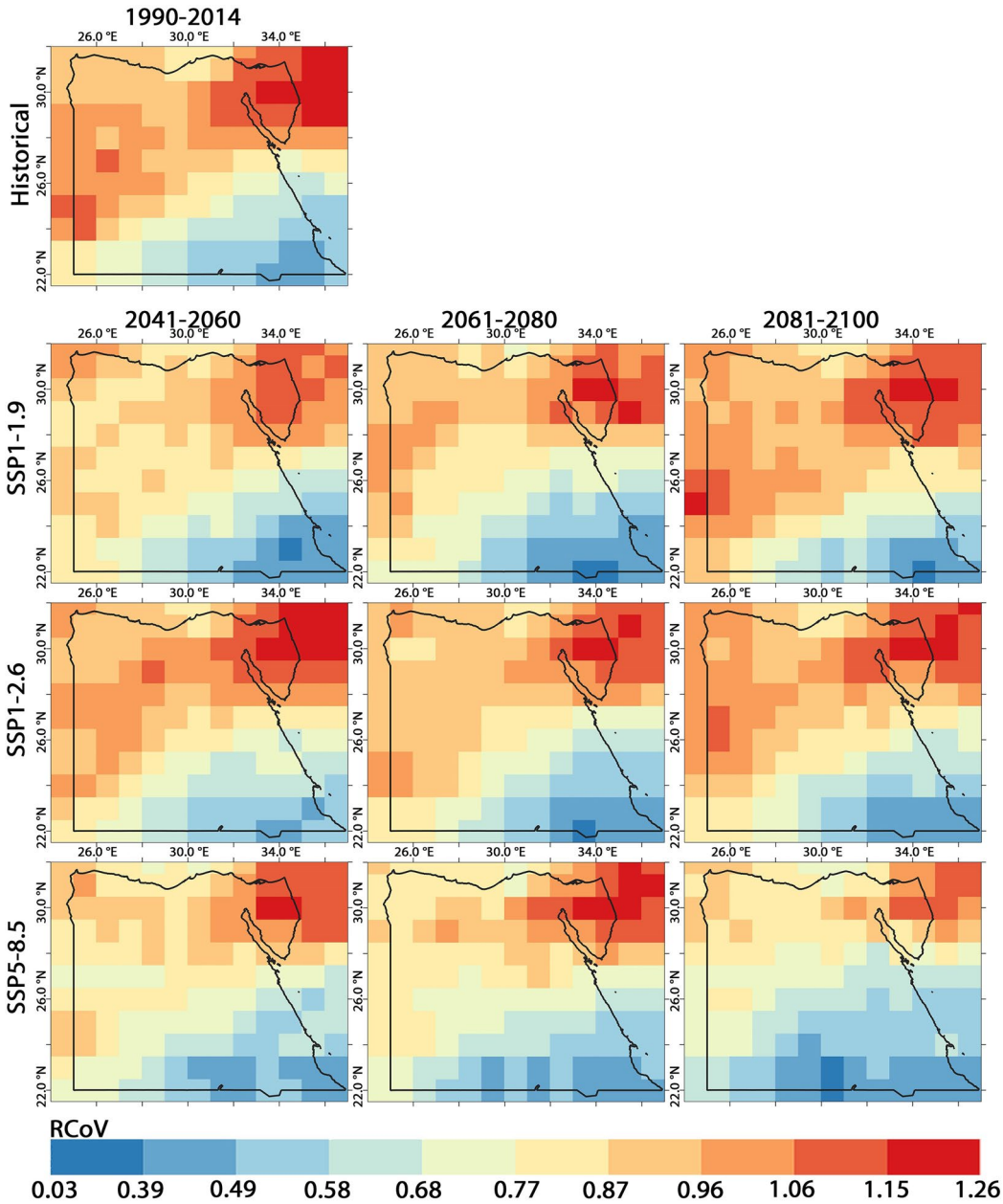

Fig. 5 The inter-annual robust coefficient of variability for the historical and future periods for different shared socioeconomic pathways (rows) during 2041–2060, 2061–2080, and 2081–2100 (columns)

ensemble. Furthermore, this study found that WPD would increase for SSP1–1.9 and 1–2.6, as well as for SSP5–8.5. The tendency of having the same direction of change in WPD with a smaller magnitude for low emission scenarios compared to high emissions one was also observed in several studies in different locations (Carvalho et al. 2021; Donk et al. 2019; Graf et al. 2019; Lima et al. 2021). This expected increase in WPD in Egypt shall give it an advantage over Europe, where several studies project a decrease in wind energy power for different SSPs (Carvalho et al. 2021; Martinez and Iglesias 2021).

Recent studies proved that the regional climate in Egypt is changing (Gado et al. 2019; Hereher 2016; Kenawy et al. 2019a, b; Nashwan et al. 2019). Since the 1980s, the consistency, severity, and length of cold and hot extremes have all increased dramatically (Kenawy et al. 2019a, b; Nashwan and Shahid 2019). Moreover, flash floods turned into prevalent events, resulting in dozens of deaths and significant economic losses (Saber et al. 2020). Although this study's findings showed that WPD would be higher for the worst-case scenario (SSP5–8.5) than low emission scenarios, keeping

global warming below the Paris climate agreement goals is vital for Egyptian energy management. Nashwan and Shahid (2022) revealed that a substantial increase in susceptibility to hydrological hazards is expected in the country, even if the global temperature increase can be maintained to the Paris climate agreements' limits. Furthermore, anthropogenic climate change at varying levels can impact Egyptian agriculture (Baig et al. 2019; El-Ramady et al. 2013; ElMassah 2013; Mahmoud 2017; Ouda et al. 2010), economy (Adly 2019; Onyeji and Fischer 1994; Strzepek 1996; Strzepek and Yates 2000; Sušnik et al. 2015; Yates and Strzepek 1998), homeland security, and public health (Brown et al. 2007; Johnstone and Mazo 2011; Lotfy 2014; Saad-Hussein et al. 2011; Werrell et al. 2015). Thus, the authors advocate the importance of keeping warming levels under the Paris climate agreement goals for Egypt, even though higher warming levels will have higher wind energetic resources.

GCMs have some limitations in assessing WPD. First, the relatively coarse spatial resolution of their outputs. Second, the absence of 100 m level wind information. GCMs only provide wind components at 10 m or on other standard pressure levels. The third limitation is that few GCMs offer hourly wind data. Karnauskas et al. (2018) demonstrated quantitatively that none of them sufficiently weaken the scientific soundness and validity or the societal value of results derived by GCMs.

Several studies employed GCMs' wind data having different spatial resolutions to estimate WPD at regional or global levels. Qian and Zhang (2021), Karnauskas et al. (2018), and Deng et al. (2021) remapped different CMIP6 GCMs' outputs to $1^\circ \times 1^\circ$. Carvalho et al. (2021) re-gridded to $1.125^\circ \times 1.125^\circ$ as it was the lowest resolution of all the available GCMs. Other studies employed coarse spatial resolution ($> 2^\circ \times 2^\circ$), mostly without stating the reason behind their choice (Akinsanola et al. 2021; Carvalho et al. 2017; Reyers et al. 2016; Zheng et al. 2019). On the other hand, studies that employed regional climate models (RCMs) mostly used finer spatial resolution of ~ 12 km (Chen 2020; Costoya et al. 2020a, b; Davy et al. 2018; Santos et al. 2018). The present study chose $1^\circ \times 1^\circ$ as it is approximately the average gridsize of the CMIP6 GCMs. Carvalho et al. (2021) highlighted that GCM usually has limitations in representing terrain features (i.e., coastlines, ground elevation, etc.), which impacts their estimation of the 10 m wind components over complex terrain. Carvalho et al. (2014) stated that GCM-simulated mesoscale wind flow is not accurate over complex terrains. However, Karnauskas et al. (2018) found that the magnitude and variability of monthly WPD calculated from NCEP/NCAR Reanalysis at $2.5^\circ \times 2.5^\circ$ grid cells were highly correlated ($r = 0.94$) to point measurements by wind towers located in complex terrain. Such a comparison cannot be made for GCMs as their simulations are not temporally synchronous with the real world. They concluded that GCM outputs at coarse spatial resolution do not undermine their use to estimate WPD. On the other hand, Egypt's land is mostly flat, as shown in Fig. S1, with few complex topology features.

The lack of wind information at the 100 m level in GCMs/RCMs possesses uncertainty in WPD estimated using extrapolated 10 m winds. Most previous studies used the power law, as the present study, to vertically offset the 10 m wind up to 100 m (the average level of turbine hub). Goddard et al. (2015) illustrated that this upward extrapolation should yield reasonable wind characteristics for WPD projections. Furthermore, Karnauskas et al. (2018) compared the total wind power generated at a wind tower at 80 m to that estimated by extrapolating 10-m data and found that power law, on average, predicts the total wind power extremely well ($r = 0.98$).

Davy et al. (2018) pointed out that the ratio of WPD calculated using 3 hourly data to that obtained using daily data ranges from 1 up to 1.4 in Egypt. Furthermore, Karnauskas et al. (2018) found that monthly total power estimated using monthly wind data underestimated the power obtained using hourly data at a global scale but still highly correlated ($r = 0.94$). Finer temporal and spatial resolution data can be considered in the future in estimating WPD at a regional scale.

Conclusions

This study is the first to explore the future changes in wind energy in Egypt using CMIP6 models. It employed an ensemble of state-of-art CMIP6 GCMs for the SSP1–1.9 and 1–2.6 and 5–8.5 scenarios that inform the Paris climate agreements' goals and the worst-case of global warming. The study estimated the projected changes for three future spans (e.g., 2041–2060, 2061–2080, and 2081–2100) in terms of WPD climatology, distribution, and intra-/inter-annual variability. The results revealed that WPD would increase at varying degrees all over Egypt for different SSPs and future periods expect for the far southeast. The highest increase in WPD would be in Winter compared to other seasons. The country's far west would experience a higher increase than other parts, leading to a comparable WPD to the current and future highest location in WPD (i.e., Gulf of Suez). But the inter-annual variability in WPD would be the highest in the Gulf of Suez for different future scenarios and periods.

The study offers useful knowledge regarding how the regional climate in Egypt may change in case to achieve the global warming goals of the Paris climate agreement. The present work's outputs may help shape future strategies for wind energy generation in Egypt. Future works may project possible changes in solar energy production in Egypt as the change in aerosol levels leads to a change in solar radiation at the ground level.

Supplementary Information The online version contains supplementary material available at https://doi.org/10.1007/s10113-023-02039-w.

Author contribution Conceptualization, M.S.N., A.M.G., and W.M.H.K.; methodology, M.S.N.; software, A.M.G. and M.S.N.; validation, M.S.N., A.M.G., W.M.H.K., and S.S.; formal analysis, S.S. and W.M.H.K.; data curation, A.M.G., and M.S.N.; writing—original draft preparation, A.M.G., M.S.N., and S.S.; writing—review and editing, S.S. and W.M.H.K.; visualization, A.M.G.; supervision, M.S.N. and W.M.H.K.; all authors have read and agreed to the published version of the manuscript.

Funding Open access funding provided by The Science, Technology & Innovation Funding Authority (STDF) in cooperation with The Egyptian Knowledge Bank (EKB).

Data availability Data analyzed in this study are available upon request from the corresponding author.

Declarations

Conflict of Interest The authors declare no competing interests.

Open Access This article is licensed under a Creative Commons Attribution 4.0 International License, which permits use, sharing, adaptation, distribution and reproduction in any medium or format, as long as you give appropriate credit to the original author(s) and the source, provide a link to the Creative Commons licence, and indicate if changes were made. The images or other third party material in this article are included in the article's Creative Commons licence, unless indicated otherwise in a credit line to the material. If material is not included in the article's Creative Commons licence and your intended use is not permitted by statutory regulation or exceeds the permitted use, you will need to obtain permission directly from the copyright holder. To view a copy of this licence, visit http://creativecommons.org/licenses/by/4.0/.

References

Abubakr H, Vasquez JC, Mahmoud K, Darwish MMF, Guerrero JM (2022) Comprehensive review on renewable energy sources in Egypt—Current Status. Grid Codes and Future Vision IEEE Access 10:4081–4101. https://doi.org/10.1109/ACCESS.2022.3140385

Adly AS (2019) Climate change and energy decision aid systems for the case of Egypt. In: Climate change and energy dynamics in the Middle East. Springer, pp 79–107. https://doi.org/10.1007/978-3-030-11202-8_4

Ahmed AS (2018) Wind energy characteristics and wind park installation in Shark El-Ouinat. Egypt Renew Sustain Energy Rev 82:734–742. https://doi.org/10.1016/j.rser.2017.09.031

Akinsanola AA, Ogunjobi KO, Abolude AT, Salack S (2021) Projected changes in wind speed and wind energy potential over West Africa in CMIP6 models. Environ Res Lett 16:044033. https://doi.org/10.1088/1748-9326/abed7a

Ayugi B, Zhihong J, Zhu H, Ngoma H, Babaousmail H et al (2021) Comparison of CMIP6 and CMIP5 models in simulating mean and extreme precipitation over. East Africa Int J Climatol 41:6474–6496. https://doi.org/10.1002/joc.7207

Baig MB, Straquadine GS, Qureshi AM, Hajiyev A, Abou Hadid AF (2019) Sustainable agriculture and food security in Egypt: implications for Innovations in agricultural Extension. In: Climate change, food security and natural resource management. Springer, pp 103–131. https://doi.org/10.1007/978-3-319-97091-2_5

Bissada D (2021) Egypt - country commercial guide. Official Website of the International Trade Administration https://www.trade.gov/country-commercial-guides/egypt-electricity-and-renewable-energy. 2022

Bloom A, Kotroni V, Lagouvardos K (2008) Climate change impact of wind energy availability in the Eastern Mediterranean using the regional climate model PRECIS Nat Hazards Earth. Syst Sci 8:1249–1257. https://doi.org/10.5194/nhess-8-1249-2008

Bourdeau-Goulet S-C, Hassanzadeh E (2021) Comparisons between CMIP5 and CMIP6 models: simulations of climate indices influencing food security, infrastructure resilience, and human health in Canada. Earth's Future 9:e2021EF001995. https://doi.org/10.1029/2021EF001995

Brown OLI, Hammill A, McLeman R (2007) Climate change as the 'new' security threat: implications for. Africa Int Affairs 83:1141–1154. https://doi.org/10.1111/j.1468-2346.2007.00678.x

Carvalho D, Rocha A, Gómez-Gesteira M, Silva Santos C (2014) WRF wind simulation and wind energy production estimates forced by different reanalyses: comparison with observed data for Portugal. Appl Energy 117:116–126. https://doi.org/10.1016/j.apenergy.2013.12.001

Carvalho D, Rocha A, Gómez-Gesteira M, Silva Santos C (2017) Potential impacts of climate change on European wind energy resource under the CMIP5 future climate projections. Renew Energy 101:29–40. https://doi.org/10.1016/j.renene.2016.08.036

Carvalho D, Rocha A, Costoya X, deCastro M, Gómez-Gesteira M (2021) Wind energy resource over Europe under CMIP6 future climate projections: what changes from CMIP5 to CMIP6. Renew Sustain Energy Rev 151:111594. https://doi.org/10.1016/j.rser.2021.111594

Chen L (2020) Impacts of climate change on wind resources over North America based on NA-CORDEX. Renewable Energy 153:1428–1438. https://doi.org/10.1016/j.renene.2020.02.090

Cook NJ (1985) The designer's guide to wind loading of building structures : part 1: background, damage survey, wind data and structural classification, vol 1. Butterworths, London

Costoya X, deCastro M, Carvalho D, Gómez-Gesteira M (2020) On the suitability of offshore wind energy resource in the United States of America for the 21st century. Appl Energy 262:114537. https://doi.org/10.1016/j.apenergy.2020.114537

Costoya X, Rocha A, Carvalho D (2020) Using bias-correction to improve future projections of offshore wind energy resource: a case study on the Iberian Peninsula. Appl Energy 262:114562. https://doi.org/10.1016/j.apenergy.2020.114562

Davy R, Gnatiuk N, Pettersson L, Bobylev L (2018) Climate Change Impacts on Wind Energy Potential in the European Domain with a Focus on the Black Sea Renewable Sustainable Energy Reviews 81:1652–1659. https://doi.org/10.1016/j.rser.2017.05.253

Deng H, Hua W, Fan G (2021) Evaluation and projection of near-surface wind speed over China based on CMIP6 models. Atmosphere 12:1062. https://doi.org/10.3390/atmos12081062

Di Sante F, Coppola E, Giorgi F (2021) Projections of river floods in Europe using EURO-CORDEX, CMIP5 and CMIP6 simulations. Int J Climatol 41:3203–3221. https://doi.org/10.1002/joc.7014

Donk P, Van Uytven E, Willems P (2019) Statistical methodology for on-site wind resource and power potential assessment under current and future climate conditions: a case study of Suriname SN. Appl Sci 1:846. https://doi.org/10.1007/s42452-019-0885-6

Effat HA (2014) Spatial modeling of optimum zones for wind farms using remote sensing and geographic information system, application in the Red Sea. Egypt Journal of Geographic Information System 6:17. https://doi.org/10.4236/jgis.2014.64032

El Kenawy AM, Lopez-Moreno JI, McCabe MF, Robaa S, Dominguez-Castro F et al (2019) Daily temperature extremes over Egypt: spatial

patterns, temporal trends, and driving forces. Atmos Res 226:219–239. https://doi.org/10.1016/j.atmosres.2019.04.030
ElMassah S (2013) Would climate change affect the imports of cereals? The Case of Egypt Handbook of Climate Change Adaptation 10:978–973
El-Ramady HR, El-Marsafawy SM, Lewis LN (2013) Sustainable agriculture and climate changes in Egypt. In: Sustainable agriculture reviews. Springer, pp 41–95. https://doi.org/10.1007/978-94-007-5961-9_2
Gado TA, El-Hagrsy RM, Rashwan IMH (2019) Spatial and temporal rainfall changes in Egypt. Environ Sci Pollut Res Int 26:28228–28242. https://doi.org/10.1007/s11356-019-06039-4
Gleixner S, Demissie T, Diro GT (2020) Did ERA5 improve temperature and precipitation reanalysis over East Africa? Atmosphere 11:996. https://doi.org/10.3390/atmos11090996
Goddard SD, Genton MG, Hering AS, Sain SR (2015) Evaluating the impacts of climate change on diurnal wind power cycles using multiple regional climate models. Environmetrics 26:192–201. https://doi.org/10.1002/env.2329
Graf M, Scherrer SC, Schwierz C, Begert M, Martius O et al (2019) Near-surface mean wind in Switzerland: climatology, climate model evaluation and future scenarios. Int J Climatol 39:4798–4810. https://doi.org/10.1002/joc.6108
Hamed MM, Nashwan MS, Shahid S (2021) Performance evaluation of reanalysis precipitation products in Egypt using fuzzy entropy time series similarity analysis. Int J Climatol 41:5431–5446. https://doi.org/10.1002/joc.7286
Hamed MM, Nashwan MS, Shahid S (2022a) Climatic zonation of Egypt based on high-resolution dataset using image clustering technique Progress in Earth and Planetary. Science 9:35. https://doi.org/10.1186/s40645-022-00494-3
Hamed MM, Nashwan MS, Shahid S (2022) Inter-comparison of historical simulation and future projections of rainfall and temperature by CMIP5 and CMIP6 GCMs over Egypt. Int J Climatol 42:4316–4332. https://doi.org/10.1002/joc.7468
Hamed MM, Nashwan MS, Shahid S, Tb Ismail, Wang X-j et al (2022) Inconsistency in historical simulations and future projections of temperature and rainfall: a comparison of CMIP5 and CMIP6 models over Southeast Asia. Atmos Res 265:105927. https://doi.org/10.1016/j.atmosres.2021.105927
Hamed MM, Nashwan MS, Shiru MS, Shahid S (2022) Comparison between CMIP5 and CMIP6 models over MENA region using historical simulations and future projections. Sustain 14:10375. https://doi.org/10.3390/su141610375
Hereher ME (2016) Time series trends of land surface temperatures in Egypt: a signal for global warming Environ Earth Sci 75 https://doi.org/10.1007/s12665-016-6024-4
IPCC (2021) Climate change 2021: the physical science basis. Contribution of working group I to the sixth assessment report of the intergovernmental panel on climate change [Masson-Delmotte V, Zhai P, Pirani A, Connors SL, Péan C, Berger S, Caud N, Chen Y, Goldfarb L, Gomis MI, Huang M, Leitzell K, Lonnoy E, Matthews JBR, Maycock TK, Waterfield T, Yelekçi O, Yu R, Zhou B (eds.)]. Cambridge University Press, Cambridge, United Kingdom and New York, NY, USA, pp 2391. https://doi.org/10.1017/9781009157896
IRENA (2022) Renewable power generation costs in 2021. International Renewable Energy Agency, Abu Dhabi
IRENA (2018) Renewable energy outlook: Egypt International Renewable Energy Agency, Abu Dhabi
Johnstone S, Mazo J (2011) Global warming and the Arab Spring Survival 53:11–17 https://doi.org/10.1080/00396338.2011.571006
Karnauskas KB, Lundquist JK, Zhang L (2018) Southward shift of the global wind energy resource under high carbon dioxide emissions. Nat Geosci 11:38–43. https://doi.org/10.1038/s41561-017-0029-9
Kenawy A, López-Moreno JI, McCabe M, Robaa S, Domínguez-Castro F et al (2019) Daily temperature extremes over Egypt: spatial patterns, temporal trends, and driving forces. Atmos Res 226:219–239. https://doi.org/10.1016/j.atmosres.2019.04.030
Lashin A, Shata A (2012) An analysis of wind power potential in Port Said. Egypt Renewable and Sustainable Energy Reviews 16:6660–6667. https://doi.org/10.1016/j.rser.2012.08.012
Lima DCA, Soares PMM, Cardoso RM, Semedo A, Cabos W et al (2021) The present and future offshore wind resource in the Southwestern African region. Clim Dyn 56:1371–1388. https://doi.org/10.1007/s00382-020-05536-4
Lotfy WM (2014) Climate change and epidemiology of human parasitosis in Egypt: a review. J Adv Res 5:607–613. https://doi.org/10.1016/j.jare.2013.06.009
Mahmoud M (2017) Impact of climate change on the agricultural sector in Egypt. In: Conventional Water Resources and Agriculture in Egypt. Springer, pp 213–227. https://doi.org/10.54609/reaser.v23i1.133
Martinez A, Iglesias G (2021) Wind resource evolution in Europe under different scenarios of climate change characterised by the novel Shared Socioeconomic Pathways. Energy Convers Manag 234:113961. https://doi.org/10.1016/j.enconman.2021.113961
Meinshausen M, Nicholls ZRJ, Lewis J, Gidden MJ, Vogel E et al (2020) The shared socio-economic pathway (SSP) greenhouse gas concentrations and their extensions to 2500. Geosci Model Dev 13:3571–3605. https://doi.org/10.5194/gmd-13-3571-2020
Nashwan MS, Shahid S (2019) Spatial distribution of unidirectional trends in climate and weather extremes in Nile river basin. Theoret Appl Climatol 137:1181–1199. https://doi.org/10.1007/s00704-018-2664-5
Nashwan MS, Shahid S (2022) Future precipitation changes in Egypt under the 1.5 and 2.0°C global warming goals using CMIP6 multimodel ensemble. Atmos Res 265:105908. https://doi.org/10.1016/j.atmosres.2021.105908
Nashwan MS, Shahid S, Abd Rahim N (2019) Unidirectional trends in annual and seasonal climate and extremes in Egypt. Theoret Appl Climatol 136:457–473. https://doi.org/10.1007/s00704-018-2498-1
Nashwan MS, Shahid S, Chung E-S (2020) High-Resolution Climate Projections for a Densely Populated Mediterranean Region Sustainability 12:3684. https://doi.org/10.3390/su12093684
Nie S, Fu S, Cao W, Jia X (2020) Comparison of monthly air and land surface temperature extremes simulated using CMIP5 and CMIP6 versions of the Beijing Climate Center climate model. Theor Appl Climatol 140:487–502. https://doi.org/10.1007/s00704-020-03090-x
NREA (2021) Introduction to new & renewable energy authority (NREA). New & Renewable Energy Authority (NREA). http://nrea.gov.eg/test/en/About/Intro. Accessed 15 Jun 2022
Onyeji SC, Fischer G (1994) An economic analysis of potential impacts of climate change in Egypt. Glob Environ Chang 4:281–299. https://doi.org/10.1016/0959-3780(94)90029-9
Ortega G, Arias PA, Villegas JC, Marquet PA, Nobre P (2021) Present-day and future climate over central and South America according to CMIP5/CMIP6 models. Int J Climatol 41:6713–6735. https://doi.org/10.1002/joc.7221
Osman ZH, Awad ML, Mahmoud TK Neural network based approach for short-term load forecasting. In: 2009 IEEE/PES Power Systems Conference and Exposition, 15–18 March 2009 2009. pp 1–8. https://doi.org/10.1109/PSCE.2009.4840035
Ouda S, Sayed M, El-Afandi G, Khalil F Developing an adaptation strategy to reduce climate change risks on wheat grown in sandy soil in Egypt. In: Meeting the challenge of sustainable development in drylands under changing climate-moving from global to local, Proceedings of the Tenth International Conference on Development of Drylands, 12–15 December 2010, Cairo, Egypt,

2011. International Dryland Development Commission (IDDC), pp 346–356
Palmer TE, Booth B, McSweeney CF (2021) How does the CMIP6 ensemble change the picture for European climate projections? Environ Res Lett 16:094042. https://doi.org/10.1088/1748-9326/ac1ed9
Perkins SE, Pitman AJ, Sisson SA (2013) Systematic differences in future 20 year temperature extremes in AR4 model projections over Australia as a function of model skill. Int J Climatol 33:1153–1167. https://doi.org/10.1002/joc.3500
Pryor S, Schoof J, Barthelmie R (2005) Climate change impacts on wind speeds and wind energy density in northern Europe: empirical downscaling of multiple AOGCMs. Climate Res 29:183–198. https://doi.org/10.3354/cr029183
Qian H, Zhang R (2021) Future changes in wind energy resource over the Northwest Passage based on the CMIP6 climate projections. Int J Energy Res 45:920–937. https://doi.org/10.1002/er.5997
Reyers M, Moemken J, Pinto JG (2016) Future changes of wind energy potentials over Europe in a large CMIP5 multi-model ensemble. Int J Climatol 36:783–796. https://doi.org/10.1002/joc.4382
Riahi K, van Vuuren DP, Kriegler E, Edmonds J, O'Neill BC et al (2017) The shared socioeconomic pathways and their energy, land use, and greenhouse gas emissions implications: an overview. Global Environ Change 42:153–168. https://doi.org/10.1016/j.gloenvcha.2016.05.009
Rogelj J, den Elzen M, Höhne N, Fransen T, Fekete H et al (2016) Paris Agreement climate proposals need a boost to keep warming well below 2 °C. Nature 534:631–639. https://doi.org/10.1038/nature18307
Rogelj J, Popp A, Calvin KV, Luderer G, Emmerling J et al (2018) Scenarios towards limiting global mean temperature increase below 1.5 °C. Nature Climate Change 8:325–332. https://doi.org/10.1038/s41558-018-0091-3
Saad-Hussein A, El-Mofty H, Hassanien M (2011) Climate change and predicted trend of fungal keratitis in Egypt. East Mediterr Health J 17:468–473. https://doi.org/10.26719/2011.17.6.468
Saber M, Abdrabo KI, Habiba OM, Kantosh SA, Sumi T (2020) Impacts of triple factors on flash flood vulnerability in Egypt: urban growth, extreme climate, and mismanagement. Geosci 10:24. https://doi.org/10.3390/geosciences10010024
Salman SA, Nashwan MS, Ismail T, Shahid S (2020) Selection of CMIP5 general circulation model outputs of precipitation for peninsular Malaysia. Hydrol Res 51:781–798. https://doi.org/10.2166/nh.2020.154
Santos F, Gómez-Gesteira M, deCastro M, Añel JA, Carvalho D et al (2018) On the accuracy of CORDEX RCMs to project future winds over the Iberian Peninsula and surrounding ocean. Appl Energy 228:289–300. https://doi.org/10.1016/j.apenergy.2018.06.086
Sawadogo W, Reboita MS, Faye A, da Rocha RP, Odoulami RC et al (2021) Current and future potential of solar and wind energy over Africa using the RegCM4 CORDEX-CORE ensemble. Climate Dyn 57:1647–1672. https://doi.org/10.1007/s00382-020-05377-1
Song YH, Nashwan MS, Chung E-S, Shahid S (2021) Advances in CMIP6 INM-CM5 over CMIP5 INM-CM4 for precipitation simulation in South Korea. Atmos Res 247:105261. https://doi.org/10.1016/j.atmosres.2020.105261
Strzepek KM (1996) Economic and social adaptations to climate change impacts on water resources: a case study of Egypt. Int J Water Resour Dev 12:229–244. https://doi.org/10.1080/07900629650041975
Strzepek KM, Yates DN (2000) Responses and thresholds of the Egyptian economy to climate change impacts on the water resources of the Nile river. Clim Change 46:339–356. https://doi.org/10.1023/a:1005603411569
Sušnik J, Vamvakeridou-Lyroudia LS, Baumert N, Kloos J, Renaud FG et al (2015) Interdisciplinary assessment of sea-level rise and climate change impacts on the lower Nile delta. Egypt Science of the Total Environment 503–504:279–288. https://doi.org/10.1016/j.scitotenv.2014.06.111
UNFCCC D (2015) 1/CP. 21, Adoption of the Paris Agreement. UN Doc. FCCC/CP/2015/10/Add. 1
Werrell CE, Femia F, Sternberg T (2015) Did we see it coming?: State fragility, climate vulnerability, and the uprisings in Syria and Egypt. SAIS Rev Int Affairs 35:29–46. https://doi.org/10.1353/sais.2015.0002
Yates DN, Strzepek KM (1998) An assessment of integrated climate change impacts on the gricultural economy of Egypt. Clim Change 38:261–287. https://doi.org/10.1023/A:1005364515266
Zheng C-w, Li X-y, Luo X, Chen X, Qian Y-h et al (2019) Projection of future global offshore wind energy resources using CMIP data. Atmos Ocean 57:134–148. https://doi.org/10.1080/07055900.2019.1624497

Publisher's note Springer Nature remains neutral with regard to jurisdictional claims in published maps and institutional affiliations.